European Journal of Pharmaceutics and Biopharmaceutics 141 (2019) 172–179

Contents lists available at ScienceDirect

European Journal of Pharmaceutics and Biopharmaceutics

journal homepage: www.elsevier.com/locate/ejpb

Research paper

Dry amorphisation of mangiferin, a poorly water-soluble compound, using mesoporous silica

Adrienn Baán[a], Peter Adriaensens[b], Joris Lammens[c], René Delgado Hernandez[d], Wim Vanden Berghe[e], Luc Pieters[f], Chris Vervaet[c], Filip Kiekens[a,*]

[a] University of Antwerp, Department of Pharmaceutical Technology and Biopharmacy, Universiteitsplein 1 2610 Wilrijk, Belgium
[b] University of Hasselt, Institute for Materials Research, Agoralaan Building D, 3590 Diepenbeek, Belgium
[c] Ghent University, Laboratory of Pharmaceutical Technology, Ottergemsesteenweg 460, 9000 Ghent, Belgium
[d] Universidad de la Habana, Instituto de Farmacia y Alimentos, 222 La Habana, Cuba
[e] University of Antwerp, Department of Biomedical Sciences, Universiteitsplein 1 2610 Wilrijk, Belgium
[f] University of Antwerp, Department of Pharmaceutical Sciences, Universiteitsplein 1 2610 Wilrijk, Belgium

ARTICLE INFO

Keywords:
Mesoporous silica
Solid dispersions
Dry amorphisation
Co-milling
Drug formulation
Solubility improvement

ABSTRACT

Mangiferin, a poorly water soluble compound, was processed via a dry amorphisation technique (ball milling) in combination with mesoporous silica to enhance the solubility of mangiferin.

The amorphous samples were prepared by mixing 1:1 (w/w) Syloid® XDP 3050 silica-mangiferin mixtures using a planetary mono mill at different milling speeds and milling times according to a 3^2 full factorial experimental design. The prepared samples were characterized for dissolution profile, particle size distribution using laser diffraction particle size analyzer, thermal characteristics using DSC, crystalline characteristics using XRD and molecular interactions using FTIR and ss-NMR. The samples were tested for stability at stress conditions (40 °C/75%RH) for up to 6 months in open and closed containers. To improve stability of the samples, mixtures of 1:1:2 mangiferin-polymer (Soluplus or HPMC)-silica samples were also prepared and analyzed.

Amorphisation of mangiferin is possible using dry amorphisation by ball milling with mesoporous silica in a short amount of time. The amorphisation rate of the samples improved with the energy input of the milling process. The samples prepared with high energy input resulted in amorphous samples and showed a better stability at the stress conditions for up to 3 months. Solubility of these samples increased from 0.32 to 0.50 mg/ml and the particle size decreased from 35.5 µm to around 7 µm. The spectral analysis suggest presence of interactions between the silica material and the compound. The amorphous stability was improved with addition of polymer, even though the solubility of the samples was lower.

1. Introduction

Due to patient convenience and compliance the preferred drug delivery route is oral administration [1]. The active pharmaceutical ingredients (API) have to possess a high bioavailability to achieve the desired therapeutic effect. The biopharmaceutical classification system divides the API's in four different groups according to their permeability and water-solubility. Class II (poor solubility, high permeability) and Class IV (poor solubility and poor permeability) compounds demonstrate a low bioavailability, which can be improved by solubility enhancement methods, such as salt formation [2,3], solid dispersions [4,5], micronisation [6] and encapsulation in cyclodextrins [7–9].

Nowadays, methods that improve the solubility of APIs by converting the crystalline form into its amorphous form are of high interest. Mostly amorphous polymer-based solid dispersions are used to achieve a good stability of the amorphous form while maintaining the solubility enhancement properties [10].

Mesoporous silica materials (MPS) gained the attention due their tunable porosity, high surface area, inertness and good biocompatibility, which makes them suitable for drug delivery. Silica based drug carrier materials are more resistant to heat, pH, mechanical stress and hydrolysis-induced degradation than many polymer materials which makes them a good alternative for traditional solid dispersions.[11] These silica materials are characterized by their pore size, which varies

* Corresponding author.
E-mail addresses: adrienn.baan@uantwerpen.be (A. Baán), peter.adriaensens@uhasselt.be (P. Adriaensens), rene.delgado@cidem.sld.cu (R. Delgado Hernandez), wim.vandenberghe@uantwerpen.be (W. Vanden Berghe), luc.pieters@uantwerpen.be (L. Pieters), chris.vervaet@ugent.be (C. Vervaet), filip.kiekens@uantwerpen.be (F. Kiekens).

https://doi.org/10.1016/j.ejpb.2019.05.026
Received 7 March 2019; Received in revised form 27 May 2019; Accepted 28 May 2019
Available online 29 May 2019
0939-6411/

between 2 and 50 nm and are randomly oriented.[12] MPS is suitable for solubility enhancement of poorly water-soluble compounds by entrapping the drugs in an amorphous form and by preventing recrystallization due to the small pore size and the interaction between the silanol groups and the drug substance [13]. The high surface area and hydrophilicity of MPS enhances the wettability which results in faster dissolution. Improvement of the stability of the amorphous form is achieved by the reduction of the Gibbs free energy due to the high surface energy of MPS [11]. In addition, the chance for nucleation and crystal growth is reduced by the constrained space [14]. Drug loading capacity of these materials are high, even up to 60% [15]. As solvent-free method, the co-milling method is a low cost and easy method for large–scale processing. Various technologies such as planetary [16], oscillatory ball mill [17] or turbula mill can be used to load drugs into the pores. The degree of amorphisation and the extent of drug loading is influenced by several parameters, such as the time and intensity of milling, or the silanol content of MPS. Several studies were performed for co-milling of API with mesoporous silica to improve the dissolution properties of the API, but in these cases the processing time was a couple of hours or even days [18–20]. Reduction of processing time still remains an important challenge to make this technology more attainable for industrial application.

The compound used in this study is a promising therapeutic polyphenol, namely mangiferin. It possesses several health improving properties, such as antiviral, anti-inflammatory, antidiabetic, analgesic, immunomodulatory and anticancer properties [21,22]. However, all these activities are hindered when the compound is administered orally due to its poor solubility, low bioavailability, and high hepatic first-pass metabolism [23,24]. Therefore, there is high need to develop a formulation that increases the solubility and bioavailability of mangiferin. Due to its poor solubility, not only in water, but in organic solvents as well, the applied technology to formulate this compound was dry amorphisation using mesoporous silica.

Molecular interactions between the compound and the silica material were evaluated as well as the amorphisation and the solubility enhancement potential of the method. Stability of the formulations at accelerated stability conditions was monitored for up to 6 months. In addition, amorphisation and stability of a ternary system including a hydrophilic polymer was evaluated.

2. Materials and methods

2.1. Materials

Mangiferin (MNG) (Fig. 1) was purchased from Shaanxi Sciphar Hi-Tech Industry (China). Syloid® XDP 3050 silica was kindly provided by Grace (Worms, Germany). The polymers, hydroxypropyl-methylcellulose (HPMC) and polyvinyl caprolactam-polyvinyl acetate-polyethylene glycol graft copolymer (Soluplus®) were purchased from Alfa Aesar (Kandel, Germany) and BASF (Ludwigshafen, Germany), respectively. The reagents for HPLC, acetonitrile and methanol, both HPLC grade, were purchased from Chem-Lab (Zedelgem, Belgium). Potassium phosphate monobasic was bought from Acros Organics (Geel, Belgium). Disodium hydrogen phosphate dehydrate and sodium dihydrogen phosphate dehydrate extra pure were purchased from Merck (Darmstadt, Germany) and sodium chloride from Carl Roth (Karlsruhe, Germany).

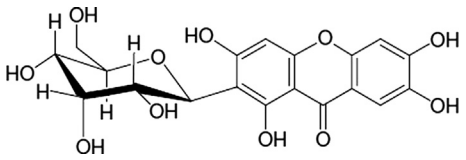

Fig. 1. Mangiferin.

2.2. Methods

2.2.1. Preparation of samples

Amorphous mangiferin samples were prepared using a Pulverisette 6 planetary mono mill (Fritsch, Oberstein, Germany). MNG and Syloid® XDP 3050 silica were mixed in a 1:1 wt ratio (total mass of 8 g) to achieve a high drug loading and the mixture was placed in a 250 mL zirconium dioxide vessel with 50 zirconium dioxide balls of 10 mm diameter. The milling speed was varied between 400 and 600 rpm, while the milling time was 1 to 20 min according to the 3^2 full factorial experimental design seen on Fig. 2. All samples were prepared once, the center point of the design (sample E) was prepared in triplicate. The resulting mass was passed through a 25 mesh sieve (opening 710 µm) and stored in a plastic container protected from light until further use.

Mangiferin, polymer (HPMC or Soluplus®) and Syloid® XDP 3050 silica were mixed in a 1:1:2 wt ratio and the mixture was processed according to a fractional design with the settings of the outer points and the middle point of the experimental design of the silica-mangiferin mixture (400 rpm/1 min, 500 rpm/10 min and 600 rpm/20 min) to evaluate the stability improvement after polymer addition to the API-silica mixture. The processing parameters and sample compositions are listed in Table 1.

An accelerated stability study at 40 °C/75% RH was performed on all samples according to the ICH guidelines [25]. Samples were tested for drug release and thermal characteristics at following time points: 0, 1, 3 and 6 months.

2.2.2. Particle size analysis

The particle size distributions of the formulated products were analysed using an integrated light-scattering instrument, Mastersizer 3000 (Malvern, United Kingdom) using the dry dispersion method with air pressure of 2 bar and 50% feeding rate.

2.2.3. Differential scanning calorimetry

The thermal properties of the powder samples were determined using a Discovery DSC25 equipment from TA Instrument (New Castle, DE, USA). Sample powders (5–10 mg) were analyzed in Tzero aluminum pans under 50 mL/min nitrogen gas purge in modulated temperature mode. The enthalpy and temperature was calibrated using an indium standard and the heat capacity was calibrated using a sapphire standard. All samples were heated from -40 to 320 °C at a 10 °C/min heating rate with a modulation of 1.6 °C/min. Determination and quantification of the melting peak was performed using the TA Instruments TRIOS software.

2.2.4. In vitro release study

The pharmaceutical performance of API as such, API/silica and API/silica/polymer formulations were evaluated using *in vitro* release studies. The dissolution profiles over a period of 1 h were measured using a modified USP apparatus 2, with 0.5 mg/ml total mangiferin concentration (200 mg formulation) in 100/200 mL of phosphate buffer with a pH of 6.8 ± 0.1, as dissolution medium at 37 ± 1 °C. 1 mL samples were withdrawn and immediately replaced with 1 mL phosphate buffer at 2, 5, 10, 15, 30, 45 and 60 min. The taken samples were centrifuged for 5 min at 5000 rpm to separate the supernatant from the undissolved particles. The samples were analyzed by means of HPLC. The experiments were conducted in triplicate. The dissolution profiles of all samples of the experimental design were compared to the dissolution profile of crystalline mangiferin using the difference factor (f_1) and the similarity factor (f_2) [26]. Generally if two curves have f_1 value below 15 and f_2 value above 50 they are considered equivalent.

2.2.5. High-pressure liquid chromatography

The API content of the dissolution samples was analyzed by HPLC-UV. The HPLC system consisted of a pump (Shimadzu LC-20AT), DAD detector (Shimadzu SPD-M20A), degasser (DGU-20A5), auto-sampler

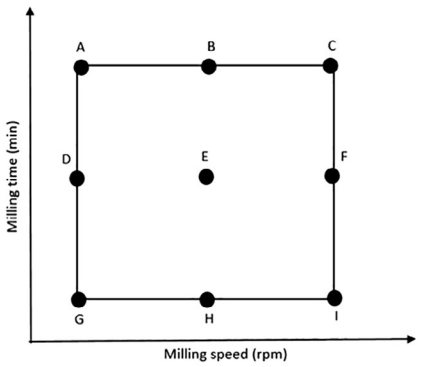

SAMPLE NAME	MILLING TIME (min)	MILLING SPEED (rpm)
Sample A	20	400
Sample B	20	500
Sample C	20	600
Sample D	10	400
Sample E	10	500
Sample F	10	600
Sample G	1	400
Sample H	1	500
Sample I	1	600

Fig. 2. Design of experiments for silica-mangiferin mixtures.

Table 1
Prepared samples for the ternary systems.

SAMPLE NAME	MILLING TIME (MIN)	MILLING SPEED (RPM)	POLYMER
Sample 1	1	400	Soluplus
Sample 2	10	500	Soluplus
Sample 3	20	600	Soluplus
Sample 4	1	400	HPMC
Sample 5	10	500	HPMC
Sample 6	20	600	HPMC

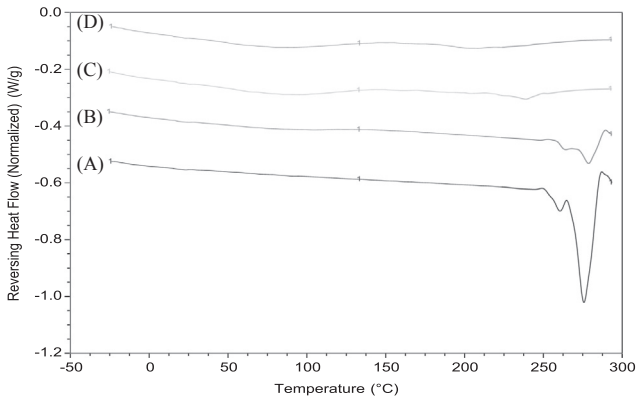

Fig. 3. DSC thermograms of (A) pure mangiferin; (B) Sample G (400 rpm, 1 min); (C) Sample E (500 rpm, 10 min) and (D) Sample C (600 rpm, 20 min).

(Shimadzu SIL-20A) and column (GraceSmart® RP18 Column 150 × 4.6 mm 5u 120A). The total flow rate was set at 1.0 mL/min and the mobile phase consisted of acetonitrile (ACN)/0.01 M KH_2PO_4 in isocratic mode with 15% ACN and 85% 0.01 M KH_2PO_4. The injection volume was 20 µL, and detection was performed at 254 nm. The integration of the peak area was performed using LC Postrun Analysis (Shimadzu), and the concentration was calculated with reference to an external calibration curve.

2.2.6. Fourier-transformation infrared spectroscopy (FTIR)

FTIR spectra of the samples were obtained using ATR-FTIR Nicolet IS5 spectrophotometer (Thermofisher, Waltham, USA). The spectra were recorded in the 4000–500 cm^{-1} region with a resolution of 4 cm^{-1} on ATR-diamond crystal. Each sample was measured in triplicate.

2.2.7. X-ray powder diffraction (XRPD)

XRPD was performed using a Siemens D5000 diffractometer (Bruker, Karlsruhe, Germany) with Cu Kα radiation (0.154 nm). An acceleration voltage of 40 kV was used. Samples were scanned between 5° and 60° 2θ with a step size of 0.02° and a step time of 1 sec/step.

2.2.8. High resolution solid-state NMR

Carbon-13 solid-state cross-polarization magic angle spinning (CP/MAS) NMR spectra were acquired on an Agilent VNMRS DirectDrive 400 MHz spectrometer (9.4T wide bore magnet) equipped with a T3HX 3.2 mm probe. Magic angle spinning was performed at 16 kHz with ceramic rotors of 3.2 mm in diameter (34 µL rotors). The aromatic signal of hexamethylbenzene was used to determine the Hartmann-Hahn condition ($\omega_{1H} = \gamma_H B_{1H} = \gamma_C B_{1C} = \omega_{1C}$) for cross-polarization, and to calibrate the carbon chemical shift scale (132.1 ppm).

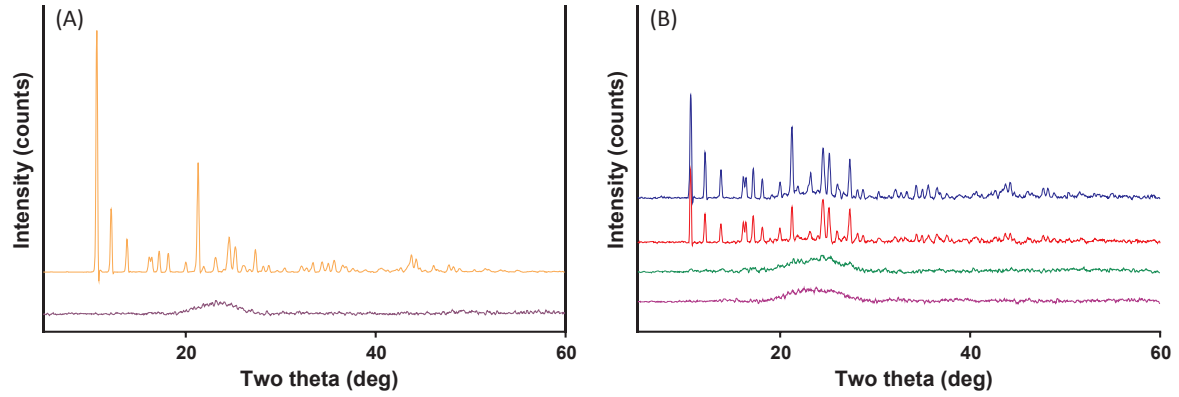

Fig. 4. The XRD patterns of crystalline mangiferin (A, orange), Syloid® XDP 3050 (A, purple); Physical mixture of Syloid® XDP 3050 and mangiferin (B, blue), and ball milled samples: the low energy milled sample (B, red), the middle point sample (B, green) and the high energy milled sample (B, purple). (For interpretation of the references to colour in this figure legend, the reader is referred to the web version of this article).

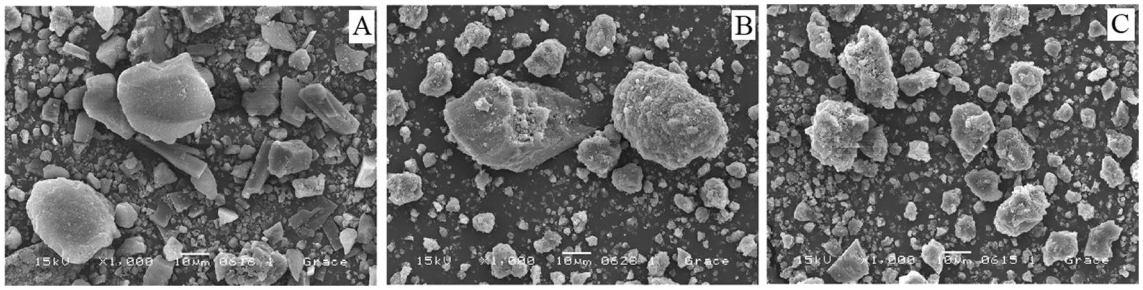

Fig. 5. SEM pictures of ball milled mangiferin-silica formulations: (A) Sample G (400 rpm, 1 min); (B) Sample E (500 rpm, 10 min); (C) Sample C (600 rpm, 20 min).

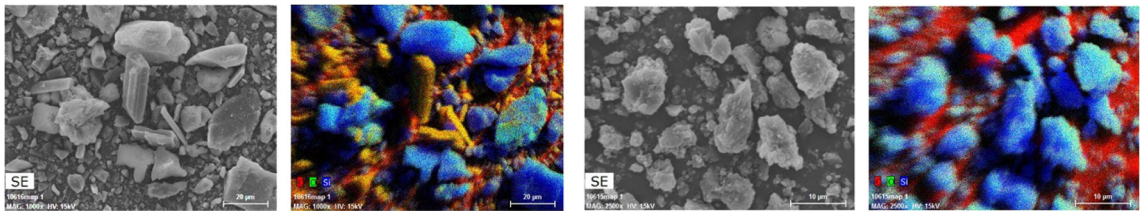

Fig. 6. SEM picture and EDX mapping of ball milled mangiferin-silica formulations: Sample G (400 rpm, 1 min) - left; Sample C (600 rpm, 20 min) - right.

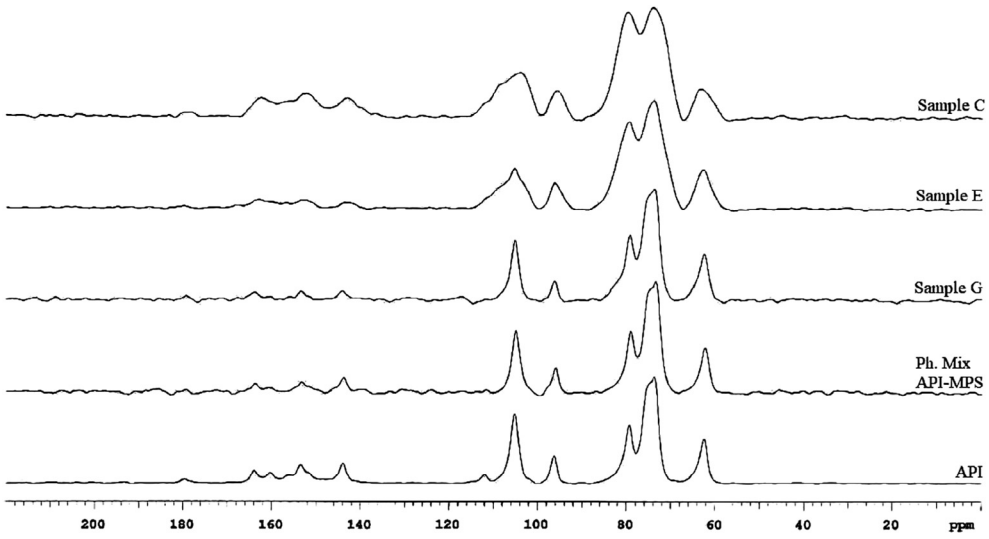

Fig. 7. ss-NMR spectra of crystalline mangiferin, physically mixed mangiferin with silica and ball milled mangiferin-silica formulations; Sample G (400 rpm, 1 min), Sample E (500 rpm, 10 min) and Sample C (600 rpm, 20 min).

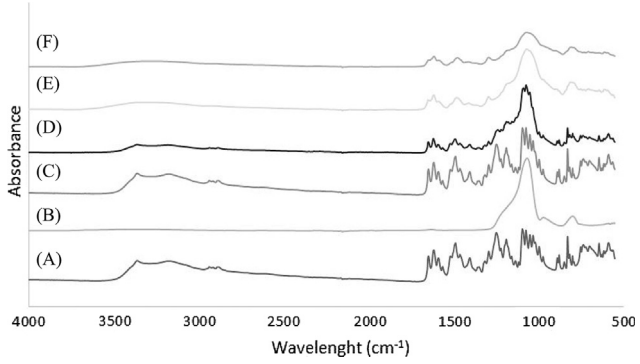

Fig. 8. FTIR spectra of (A) mangiferin, (B) mesoporous silica, (C) physical mixture of mangiferin-silica, ball milled mangiferin-silica formulations: (D) Sample G (400 rpm, 1 min); (E) Sample E (500 rpm, 10 min) and (F) Sample C (600 rpm, 20 min).

Table 2
Difference factors and Similarity factors of the dissolution profiles of ball milled mangiferin-silica samples.

SAMPLE NAME	f_1 value (%)	f_2 value (%)
Sample A	66.8	24.9
Sample B	67.1	24.6
Sample C	93.2	17.7
Sample D	60.1	27.2
Sample E	68.5	24.4
Sample F	62.0	26.2
Sample G	14.9	51.9
Sample H	10.2	57.7
Sample I	7.7	69.7

Acquisition parameters used were the following: a spectral width of 50 kHz, a 90° pulse length of 2.5 μs, a spin-lock field for CP of 75 kHz, a contact time for CP of 2 ms, an acquisition time of 25 ms and a recycle delay time of 5 s. High power proton dipolar decoupling during the acquisition time was set to 100 kHz.

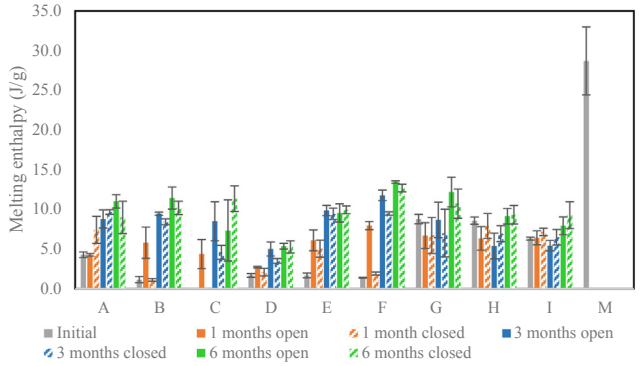

Fig. 9. The melting enthalpies of (M) mangiferin and binary samples stored at accelerated storage conditions up to 6 months.

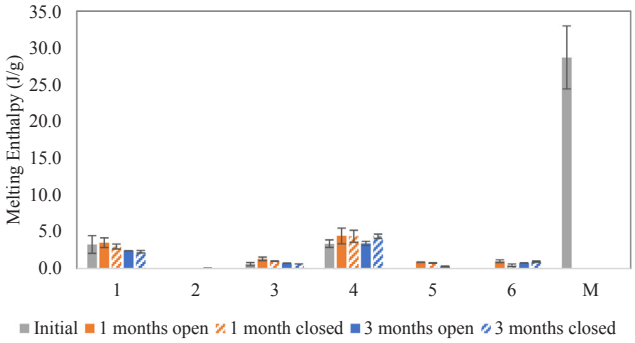

Fig. 11. The melting enthalpies of (M) mangiferin and ternary samples stored at accelerated storage conditions during 3 months.

2.2.9. Scanning electron microscope (SEM)

SEM measurements were performed using a Jeol JSM 6380 (Jeol, Japan) on gold/palladium sputtered samples in order to analyze the morphology. Energy-dispersive X-ray analysis was performed with the use of Quantax set (Bruker, USA) to determine the element composition of the samples. By scanning the electron beam across the sample surface and detecting the emitted x-rays from each pixel, the elemental distribution can be point located and related to the SEM image [27].

3. Results and discussion

3.1. Syloid® XDP 3050 silica-mangiferin formulations

3.1.1. Solid state properties of formulations

Mangiferin was in its crystalline state before processing as it is shown on the DSC thermogram by an endothermic peak around 275 °C (Fig. 3). Amorphisation of mangiferin was achieved after 20 min of processing in the planetary mono mill with a milling speed of 600 rpm. The processing time was significantly shorter than that of already reported co-milling experiments ranging from 3 h to 12 h. [16,28–30]. While ball milling of API's as such can decrease the particle size and affect the specific surface area and particle shape [31], it also can lead to amorphisation of the compound [32]. The conversion into crystalline

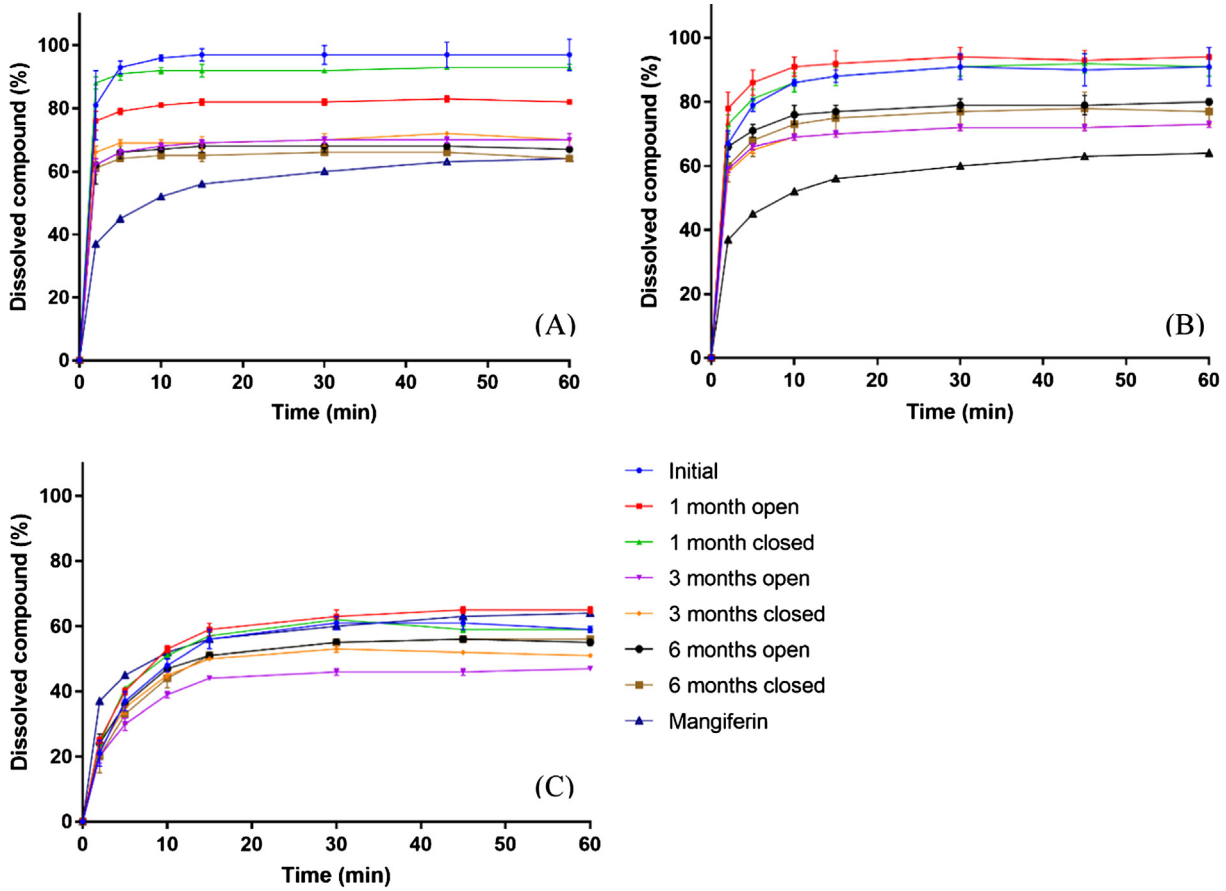

Fig. 10. Dissolution profiles of (A) Sample C, (600 rpm, 20 min) (B) Sample E (500 rpm, 10 min) and (C) Sample G (400 rpm, 1 min) compared to the dissolution profile of mangiferin followed in stability evaluation.

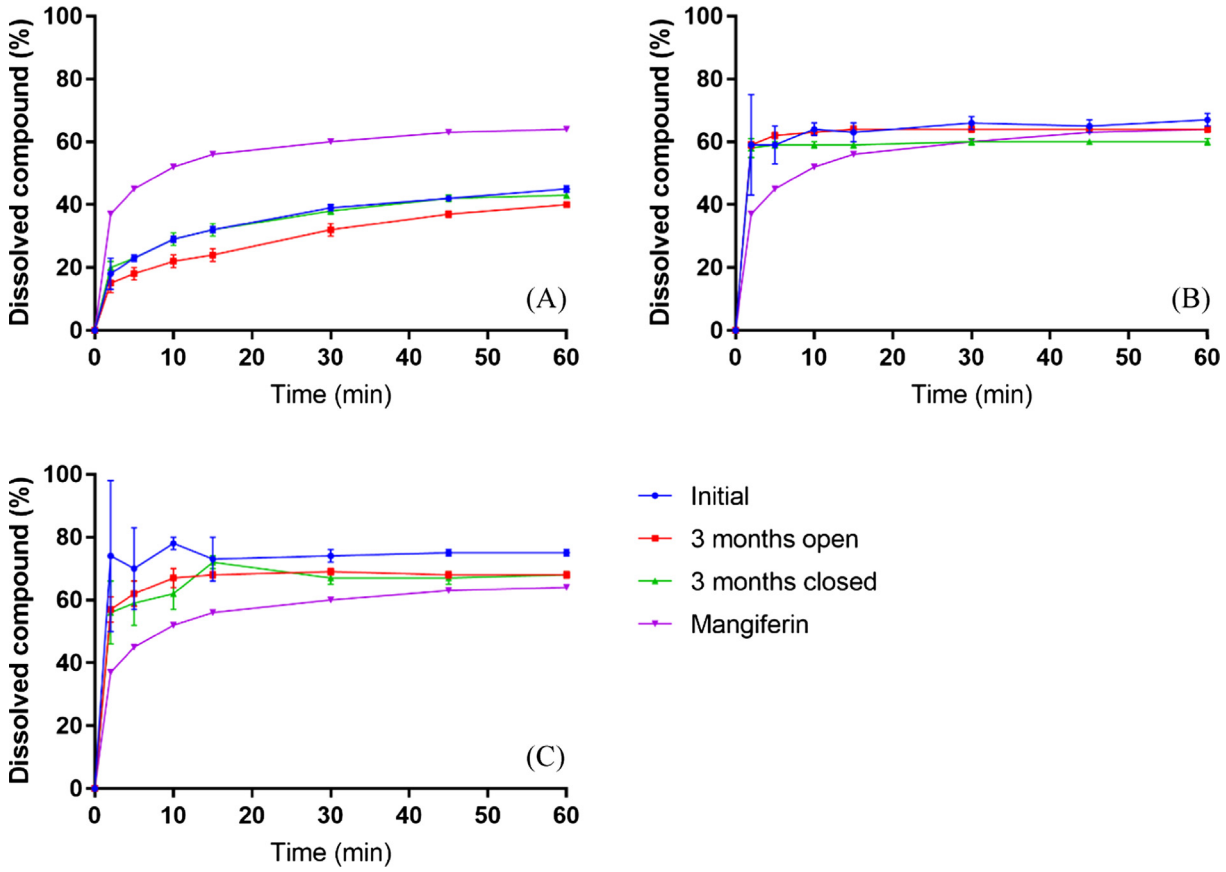

Fig. 12. Dissolution profiles of samples with HPMC compared with that of pure mangiferin: (A) Sample 4 (400 rpm , 1 min); (B) Sample 5 (500 rpm, 10 min); (C) Sample 6 (600 rpm, 20 min).

form usually happens spontaneously after processing as a result of thermodynamic instability of disordered systems. Stability of the amorphous form can be increased by using binary systems with hydrophilic excipients, like polymers. The properties of the used excipient strongly affect the performance and the quality of the drug formulation, therefore appropriate drug-carrier combination selection is needed. Using mesoporous silica in combination with certain compounds can shorten the processing time for amorphisation by intermolecular interaction due to the surface hydroxyl groups. The amorphous nature of mangiferin in ball milled silica formulation with high energy processing (Sample C) was confirmed by the absence of the endothermic melting peak. The middle point samples (Sample E) showed almost complete amorphisation with melting point temperature reduction of the remaining crystalline fraction. In case of low energy processing (Sample G) the endothermic peak was reduced, but complete amorphisation was not achieved. The reduction of peak enthalpy and temperature is due to the immobilization by strong chemical interactions between mangiferin and silica material [33]. Due to the silanol groups present on the surface of the silica material and the hydroxyl groups present in mangiferin, formation of hydrogen bonds are likely.

The X-ray diffractograms of the crystalline mangiferin and the Syloid® XDP 3050 are given in Fig. 4A. The crystalline diffraction pattern shows characteristic peaks for mangiferin, while the diffractogram of the silica material suggests an amorphous structure. On Fig. 4B the X-ray diffractograms of the physical mixture, the middle and the two outer points of the design are presented. For the physical mixture and the low energy milled sample (Sample G) the characteristic peaks of the mangiferin are still present, while in case of the high energy milled sample (Sample C) the diffraction pattern shows a halo, suggesting the presence of amorphous material. In case of the middle point sample (Sample E) peaks are still present in the halo shown on the diffractogram, corresponding to the partial amorphisation. These results confirm the results of the DSC analysis.

Physical mixture samples had an average particle size of 35.5 μm before processing. The high energy milling process resulted in particles with a particle size around 7 μm, while low energy processing did not affect the particles size. In case of the low energy milled samples porosity did not change significantly, the silica structure stayed stable and the particles were only partially filled with mangiferin. With high energy milling complete filling of the pores was achieved. The porosity and the pore volume of the samples change as well, as due to the milling process the pores collapsed. This hypothesis regarding the porosity changes was verified and confirmed using N_2 physisorption measurements (data not shown).

The SEM pictures (Fig. 5) confirmed the reduction of particle size at higher milling time and rotation speed. It is also clear that in case of low energy milling, the mangiferin crystals are still present, while at high energy milling, complete dispersion of mangiferin in the pores of silica is achieved (Fig. 6). While in case of the low energy milling the mangiferin crystals ([1]yellow) are still numerously present next to the silica particles (blue), in case of the high energy milling only the silica particles (blue) are visualized.

3.1.2. Molecular interaction between silica and mangiferin

To understand the interaction between mangiferin and mesoporous silica ^{13}C solid-state NMR and Fourier transformation infrared spectroscopy were performed. NMR spectra are shown in Fig. 7. The difference in the chemical shifts (peak position) of the NMR peaks between

[1] For interpretation of color in Fig. 6, the reader is referred to the web version of this article.

crystalline and amorphous state was not significant. Broadening of the peaks was more remarkable in case of the sample prepared by high energy milling. The broadening of the peaks can be explained by the amorphisation of mangiferin, which enables a broader distribution of molecular orientation [13]. The peak shapes clearly differ between the low energy (Sample G) and high energy milling (Sample C). The presence of sharp peaks in the spectrum of the physical mixture and Sample G suggest that crystalline mangiferin is present in the system.

The Fourier transformation infrared spectra are shown in Fig. 8. In the spectrum of the mesoporous silica material, a broad band can be observed around 1060 cm^{-1} which corresponds to the asymmetric stretching of Si—O—Si bond. The peak around 800 cm^{-1} is due to the symmetric stretching vibration of the Si—O bond while the band at 960 cm^{-1} corresponds to the symmetric Si—OH. The spectrum of crystalline mangiferin shows a broad absorption band around 3373 cm^{-1} corresponding to the hydroxyl groups, while around 2933 cm^{-1} the absorption band of the asymmetric C—H stretching can be observed. The signals of the aromatic nucleus are shown around 1622 cm^{-1}. As the energy of milling increases, major changes occur in the region 1600–800 cm^{-1} in case of the ball milled samples. The intensity of the signals of the aromatic conjugated carbonyl groups (1651 cm^{-1}) together with signals of the aromatic nucleus (1622 cm^{-1}) alter after the incorporation of mangiferin in the mesoporous silica. These signals are getting broader with the increasing energy of the milling. Due to the molecular interaction between mangiferin and the mesoporous silica, also the absorption band (3373 cm^{-1}) of the hydroxyl groups of mangiferin flattens out proportionally with the energy provided to the samples during milling. This provides another confirmation for the formation of hydrogen bonds between the silanol groups of the mesoporous silica and the hydroxyl groups of mangiferin.

3.1.3. In vitro release study

Crystalline mangiferin showed a dissolved concentration of 0.183 mg/ml after 2 min and 0.321 mg/ml after 60 min. Low energy milling did not improve the dissolution profile of mangiferin, these samples had a dissolved concentration of 0.104 mg/ml after 2 min and 0.305 mg/ml after 60 min. In contrary, the high energy milled samples (Sample C) had an increased dissolution rate and solubility with 0.405 mg/ml concentration after 2 min and 0.491 mg/ml dissolved mangiferin after 60 min. The difference and similarity factors are presented in Table 2. All samples processed during at least 10 min by ball milling improved the dissolution profile of mangiferin.

3.1.4. Stability of the formulations

According to the DSC results only one sample was still completely amorphous after 1 month storage, the high energy milled sample (Sample C) in closed storage conditions. This sample showed signs of recrystallisation after one month in open conditions. Samples stored in open container showed a higher rate of recrystallisation than the samples stored in closed containers. Due to the high humidity conditions in an open container, the amorphous mangiferin molecules, which are not interacting with the silica material, convert back to the crystalline form due to the solubilizing effect of water. The water molecules go also into competition with the hydroxyl groups of mangiferin to form hydrogen bonds with the silanol groups. Due to competition, the water molecules are driving the mangiferin molecules, which are in molecular interaction with the silica material, out of the pores of mesoporous silica. Outside of the pores the mangiferin molecules can easily recrystallize as no more hindering is present. After 3 months all samples showed recrystallisation in open and closed conditions as well. The enthalpies of the melting peaks of the samples can be seen on Fig. 9. After 6 months storage all sample reached a melting enthalpy around 10 J/g which is around 50% crystalline material, except sample D which had processing parameters of 400 rpm and 10 min milling.

The dissolution profiles were also compared. In case of high energy milled samples a decrease in total dissolved compound in 60 min can be seen, from 0.505 mg/ml it decreased after 6 months storage to 0.325 mg/ml in open and 0.340 mg/ml in closed conditions which can be explained by the recrystallisation of the compound in the formulation, but the dissolution rate was still significantly higher than that of crystalline mangiferin, 0.310 mg/ml after 2 min independent of storage conditions compared to the 0.183 mg/ml of mangiferin. The samples with low energy milling showed a lower dissolution rate and a lower total dissolved amount of mangiferin after 6 months storage independent of storage condition than crystalline mangiferin. Dissolution profiles of high energy milling and low energy milling can be seen on Fig. 10.

3.2. Syloid®XDP 3050 silica-polymer-mangiferin formulations

Preparation of ternary systems using mesoporous silica-API-polymer systems can improve amorphisation of the API and also the stability of the amorphous form in the formulation. A higher amorphisation rate was confirmed as even at low milling settings a higher amorphisation rate was achieved (11.5 ± 0.5% crystalline compound content) compared to the binary formulation (30.5 ± 1% crystalline compound content). These samples remained amorphous during storage, since no significant changes were observed during stability evaluation independent of the processing parameters (Fig. 11). Sample 2 was amorphous even after 3 months storage, while sample 3, 5 and 6 had less than 3.5% crystalline mangiferin in the formulation. Slight decrease can be observed in crystallinity for the samples stored in open container. Interaction between polymers, silica material and API needs to be further examined to be able to properly understand the reason of the decrease in crystallinity during storage.

When looking at the dissolution profile these samples had an initial solubility which was lower than that of the binary systems independent of the preparation parameters. The samples prepared with Soluplus as polymer component showed a similar solubility compared to crystalline mangiferin, even with high energy milling. Low energy milled samples showed a reduced solubility with only 0.148 mg/ml dissolved mangiferin after 60 min. In the observed time frame these samples did not reach steady-state solubility yet. The dissolution profile of these samples did not change significantly during stability evaluation. In case of the HPMC samples an improvement of solubility could be observed with increased milling energy on Fig. 12, the low energy milled sample (sample 4) had a solubility of 0.226 mg/ml, the middle point sample (sample 5) had a solubility of 0.335 mg/ml while the sample with high energy milling had a solubility of 0.373 mg/ml. In these cases the dissolution rate was also increased, 0.326 mg/ml mangiferin was dissolved after 2 min. After 3 months stability evaluation the dissolution profile of the low energy milled samples did not change, while the high energy milled samples showed similar dissolution profile as the binary samples prepared with the same ball mill settings. For the high energy milled samples solubility was still slightly higher than that of crystalline mangiferin with 0.344 mg/ml in open and closed conditions.

4. Conclusion

The results showed that – depending on the settings during ball milling – molecular interactions were present between mesoporous silica and mangiferin, resulting in an amorphous system with increased solubility. This amorphisation was achieved in already 20 min, which was significantly faster than previously reported. In comparison with other solubility enhancement methods, a high drug loading in the mesoporous silica was achieved and no organic solvent was needed during sample preparation. Addition of polymer enhanced the amorphisation rate of the samples and improved their stability.

Acknowledgement

Many thanks to everyone involved in this research. We specifically

thank Fred Monsuur (W. R. Grace & co., Worms, Germany) for the scientific support and discussions and for providing us the SEM/SEM-EDX pictures. This project is part of an International collaboration (VLIR-UOS (Belgium) TEAM project no. ZEIN2016PR418).

References

[1] K.K. Jain, Current Status and Future Prospects of Drug Delivery Systems, Humana Press, New York, NY, 2014.
[2] A.T.M. Serajuddin, Salt formation to improve drug solubility, Adv. Drug Deliv. Rev. 59 (2007) 603–616, https://doi.org/10.1016/j.addr.2007.05.010.
[3] H. Lieberman, N.M. Vemuri, Chemical and Physicochemical Approaches to Solve Formulation Problems, Elsevier Ltd, 2015.
[4] D.N. Bikiaris, Solid dispersions part I: recent evolutions and future opportunities in manufacturing methods for dissolution rate enhancement of poorly water-soluble drugs, Exp. Opin. Drug Deliv. (2014), https://doi.org/10.1517/17425247.2011.618181.
[5] A. Paudel, M. Geppi, G. Van Den Mooter, Structural and dynamic properties of amorphous solid dispersions: the role of solid-state nuclear magnetic resonance spectroscopy and relaxometry, J. Pharm. Sci. 103 (2014) 2635–2662, https://doi.org/10.1002/jps.23966.
[6] K.R. Vandana, Y. Prasanna Raju, V. Harini Chowdary, M. Sushma, N. Vijay Kumar, An overview on in situ micronization technique – an emerging novel concept in advanced drug delivery, Saudi Pharm. J. 22 (2014) 283–289, https://doi.org/10.1016/j.jsps.2013.05.004.
[7] T. Loftsson, P. Jarho, M. Másson, T. Järvinen, A. Publications, Expert opinion on drug delivery cyclodextrins in drug delivery, Exp. Opin. Drug Deliv. 2 (2005) 329–357, https://doi.org/10.1517/17425247.2.1.335.
[8] M.E. Brewster, T. Loftsson, Cyclodextrins as pharmaceutical solubilizers, Adv. Drug Deliv. Rev. 59 (2007) 645–666, https://doi.org/10.1016/j.addr.2007.05.012.
[9] A. Vyas, S. Saraf, S. Saraf, Cyclodextrin based novel drug delivery systems, J. Incl. Phenom. Macrocycl. Chem. 62 (2008) 23–42, https://doi.org/10.1007/s10847-008-9456-y.
[10] D. Douroumis, A. Fahr, Drug delivery strategies for poorly water-soluble drugs, First edit, John Wiley & Sons Ltd., 2013.
[11] Y. Choudhari, H. Hoefer, C. Libanati, F. Monsuur, W. Mccarthy, Mesoporous silica drug delivery systems, Amorph. Solid Dispersions. (2014) 665–693, https://doi.org/10.1007/978-1-4939-1598-9.
[12] K.S.W. Sing, D.H. Everett, R.A.W. Haul, L. Moscou, R.A. Pierotti, J. Rouquérol, T. Siemieniewska, Reporting physisorption data for gas/solid systems with special reference to the determination of surface area and porosity, Pure Appl. Chem. 57 (1985) 603–619.
[13] F.G. Vogt, K. Roberts-Skilton, S.A. Kennedy-Gabb, A solid-state NMR study of amorphous ezetimibe dispersions in mesoporous silica, Pharm. Res. 30 (2013) 2315–2331, https://doi.org/10.1007/s11095-013-1075-7.
[14] T. Limnell, T. Heikkilä, H.A. Santos, S. Sistonen, S. Hellstén, T. Laaksonen, L. Peltonen, N. Kumar, D.Y. Murzin, M. Louhi-Kultanen, J. Salonen, J. Hirvonen, V.P. Lehto, Physicochemical stability of high indomethacin payload ordered mesoporous silica MCM-41 and SBA-15 microparticles, Int. J. Pharm. 416 (2011) 242–251, https://doi.org/10.1016/j.ijpharm.2011.06.050.
[15] T. Heikkilä, J. Salonen, J. Tuura, N. Kumar, T. Salmi, D.Yu. Murzin, M.S. Hamdy, G. Mul, L. Laitinen, A.M. Kaukonen, J. Hirvonen, V.-P. Lehto, Evaluation of mesoporous TCPSi, MCM-41, SBA-15, and TUD-1 materials as API carriers for oral drug delivery, Drug Delivery 14 (6) (2007) 337–347, https://doi.org/10.1080/10717540601098823.
[16] E. Dudognon, J.F. Willart, V. Caron, F. Capet, T. Larsson, M. Descamps, Formation of budesonide/α-lactose glass solutions by ball-milling, Solid State Commun. 138 (2006) 68–71, https://doi.org/10.1016/j.ssc.2006.02.007.
[17] K. Löbmann, C. Strachan, H. Grohganz, T. Rades, O. Korhonen, R. Laitinen, Co-amorphous simvastatin and glipizide combinations show improved physical stability without evidence of intermolecular interactions, Eur. J. Pharm. Biopharm. 81 (2012) 159–169, https://doi.org/10.1016/j.ejpb.2012.02.004.
[18] L. Maggi, A. Canobbio, G. Bruni, G. Musitelli, U. Conte, Improvement of the dissolution behavior of gliclazide, a slightly soluble drug, using solid dispersions, J. Drug Deliv. Sci. Technol. 26 (2015) 17–23, https://doi.org/10.1016/j.jddst.2015.01.002.
[19] D. Bahl, J. Hudak, R.H. Bogner, Comparison of the ability of various pharmaceutical silicates to amorphize and enhance dissolution of indomethacin upon co-grinding, Pharm. Dev. Technol. 13 (2008) 255–269, https://doi.org/10.1080/10837450802012869.
[20] D. Bahl, R.H. Bogner, Amorphization of indomethacin by Co-grinding with neusilin US2: amorphization kinetics, physical stability and mechanism, Pharm. Res. 23 (2006) 2317–2325, https://doi.org/10.1007/s11095-006-9062-x.
[21] H. Liu, R. Tong, X. He, Y. Wang, T. Lei, S. Du, X. Xie, H. Wang, Mangiferin: an effective therapeutic agent against several disorders (Review), Mol. Med. Rep. (2018) 4775–4786, https://doi.org/10.3892/mmr.2018.9529.
[22] D. García-Rivera, R. Delgado, N. Bougarne, G. Haegeman, W. Vanden Berghe, Gallic acid indanone and mangiferin xanthone are strong determinants of immunosuppressive anti-tumour effects of Mangifera indica L. bark in MDA-MB231 breast cancer cells, Cancer Lett. 305 (2011) 21–31, https://doi.org/10.1016/j.canlet.2011.02.011.
[23] M. Imran, M.S. Arshad, M.S. Butt, J. Kwon, M.U. Arshad, M.T. Sultan, Mangiferin: a natural miracle bioactive compound against lifestyle related disorders, Lipids Health Dis. 16 (2017) 1–17, https://doi.org/10.1186/s12944-017-0449-y.
[24] S. Saha, P. Sadhukhan, P. Sil, C. Mangiferin, A xanthonoid with multipotent anti-inflammatory potential, BioFactors 42 (2016) 459–474, https://doi.org/10.1002/biof.1292.
[25] ICH Harmonized Tripartite Guideline: Stability testing of New Drug Substances and Products Q1A (R2), in: Int. Conf. Harmon. Tech. Requir. Regist. Pharm. Hum. Use, 2003.
[26] J.W. Moore, H.H. Flanner, Mathematical comparison of dissolution profiles, Pharm. Technol. 20 (1996) 64–75.
[27] N. Sandler, N. Genina, E. Wisaeus, J. Rantanen, D. Raijada, J. Peltonen, D. Fors, A step toward development of printable dosage forms for poorly soluble drugs, J. Pharm. Sci. 102 (2013) 3694–3704, https://doi.org/10.1002/jps.23678.
[28] J. Szafraniec, A. Antosik, J. Knapik-Kowalczuk, M. Kurek, K. Syrek, K. Chmiel, M. Paluch, R. Jachowicz, Planetary ball milling and supercritical fluid technology as a way to enhance dissolution of bicalutamide, Int. J. Pharm. 533 (2017) 470–479, https://doi.org/10.1016/j.ijpharm.2017.03.078.
[29] P. Nowak, A. Krupa, K. Kubat, A. Węgrzyn, H. Harańczyk, A. Ciułkowska, R. Jachowicz, Water vapour sorption in tadalafil-Soluplus co-milled amorphous solid dispersions, Powder Technol. 346 (2019) 373–384, https://doi.org/10.1016/j.powtec.2019.02.010.
[30] M.L. Branham, T. Moyo, T. Govender, Preparation and solid-state characterization of ball milled saquinavir mesylate for solubility enhancement, Eur. J. Pharm. Biopharm. 80 (2012) 194–202, https://doi.org/10.1016/j.ejpb.2011.08.005.
[31] Z.H. Loh, A.K. Samanta, P.W. Sia Heng, Overview of milling techniques for improving the solubility of poorly water-soluble drugs, Asian J. Pharm. Sci. 10 (2014) 255–274, https://doi.org/10.1016/j.ajps.2014.12.006.
[32] V.V. Boldyrev, Mechanochemistry and mechanical activation of solids, Russ. Chem. Rev. 75 (2006) 177–189, https://doi.org/10.1070/RC2006v075n03ABEH001205.
[33] G. Buntkowsky, H. Breitzke, A. Adamczyk, F. Roelofs, T. Emmler, E. Gedat, B. Grünberg, Y. Xu, H.H. Limbach, I. Shenderovich, A. Vyalikh, G. Findenegg, Structural and dynamical properties of guest molecules confined in mesoporous silica materials revealed by NMR, Phys. Chem. Chem. Phys. 9 (2007) 4843–4853, https://doi.org/10.1039/b707322d.